J. Synchrotron Rad. (1998). **5**, 705–707

(Ta/Si) multilayer as a wide-bandpass monochromator material

Y. J. Park,[a]* H. S. Youn,[a] S. Banerjee,[a] D. R. Lee,[b] H. M. Baik,[b] K.-B. Lee,[b] K. J. Kim[c] and D. W. Moon[c]

[a]Beamline Research Division, Pohang Accelerator Laboratory, POSTECH, Pohang 790-784, Korea, [b]Department of Physics, POSTECH, Pohang 790-784, Korea, and [c]Surface Analysis Group, Korea Research Institute of Standards and Science, Daejon 305-606, Korea. E-mail: pjun@vision.postech.ac.kr

(*Received 4 August 1997; accepted 24 December 1997*)

Specular and non-specular X-ray reflectivity intensities of a $(Ta/Si)_{60}$ multilayer sample were measured to characterize its interface structure. Since the multilayer has a good reflectance at its multilayer peaks, its performance as a wide-bandpass monochromator for X-ray scattering experiments of polymers has been tested.

Keywords: (Ta/Si) multilayers; X-ray reflectivity; interface morphology; wide-bandpass monochromators.

1. Introduction

Synthetic multilayers are becoming more important as synchrotron radiation optical components for third-generation light sources since their typical energy bandwidth matches that of undulator radiation (Ziegler, 1995; Deschamps *et al.*, 1995). They can be used as wide-bandpass monochromators to provide a large flux of X-rays for small-angle scattering, fluorescence and time-resolved studies (Stephenson, 1988) or as power filters to reduce thermal loads of downstream monochromator crystals (Kortright & Di Gennaro, 1989).

For optical components reflectance is one of the most critical parameters determining their performances. Reflectances of these multilayers are related to their structures and, especially, to the coherent effects originating from their modulated structures. The effects of interfaces in the multilayers become more important as the periods of the multilayers reduce to a few nanometers. Intermixing widths due to the interdiffusion of atoms across the interfaces reduce the reflectance. Interface roughness is also one of the most important parameters affecting the performances of multilayer mirrors. It causes non-specular reflection and reduces specular reflection intensities. It has been known that the correlated interface roughness in multilayers results in broad resonant diffuse-scattering (RDS) peaks near multilayer Bragg peaks which cause diffuse halos around the projected images (Phang *et al.*, 1992). Therefore, it is very important to obtain sharp and smooth interfaces in multilayers for high-performance X-ray mirrors.

Multilayers including Mo/Si and W/C multilayers are widely used as soft X-ray mirrors (Salashchenko *et al.*, 1995). For hard X-rays of wavelengths less than 2 Å, grazing-incidence reflectivities higher than 70% have been reported for W/Si, W/C, W/B_4C, Ni/B_4C and other multilayers (Ziegler, 1995). Some of them are already commercially available. They can be used as condensing optical components to focus X-rays into spot sizes of micrometres. Atomic structures of these multilayers are mostly amorphous or polycrystalline and, as a result, most of them show some aging effects, mainly due to the atomic rearrangements at the interfaces. Hence, it is important to characterize their interface morphology in order to understand their aging mechanisms.

Recently it has been reported that formation of silicide is suppressed up to 973 K (which is higher than normal temperatures of optical components with proper cooling) for (Ta/Si) systems grown by ion-beam-assisted evaporation (Kwak *et al.*, 1997). Concurrent ion bombardment during deposition is expected to reduce columnar structure due to the increased adatom mobility, resulting in suppressed silicide formation. We report here our results on the characterization of the interface morphology of a $(Ta/Si)_{60}$ multilayer grown by ion-beam sputtering deposition, which is also expected to provide increased adatom mobilities, and its performance as a monochromator material for small-angle X-ray scattering (SAXS) experiments.

2. Characterization of a $(Ta/Si)_{60}$ multilayer

In this work a pair of the multilayers were grown on flat Si(100) wafers in an ion-beam-assisted sputtering chamber at the Korea Research Institute of Standards and Science (KRISS). The bilayer thickness, d, was 37 Å and the Ta layer thickness was $0.56d$. The multilayers were characterized by measuring specular and non-specular reflectivities using 1.608 Å radiation at Pohang Light Source (PLS) beamline 3C2. The reflectivity intensities were normalized by the direct beam intensities. Fig. 1 shows the reflectivity intensities on a logarithmic scale for the (*a*) specular and (*b*) non-specular condition with an offset angle of 0.1°. The first-order multilayer peak occurs at $2\theta = 2.58°$ with a reflectivity of 54%. The peak has a full width at half-maximum of $\Delta 2\theta = 0.09°$, corresponding to $\Delta E/E \simeq 3.5 \times 10^{-2}$. The total interfacial width including both intermixing width and interface roughness was estimated from the specular reflectivity intensities using Parratt's recursive relation (Parratt, 1954). The estimated values of the interfacial widths are 2.30 and 3.08 Å for Ta-on-Si interfaces (*A*-type interfaces) and Si-on-Ta interfaces (*B*-type interfaces), respectively.

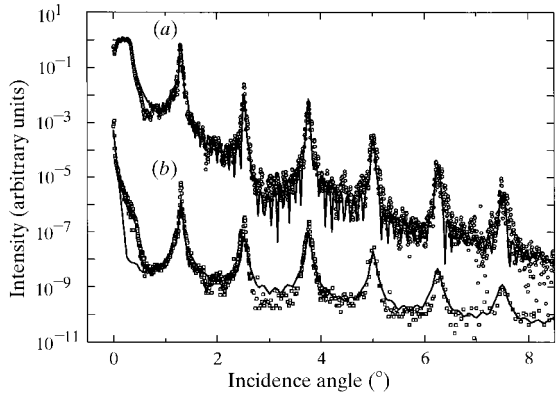

Figure 1
Measured reflectivity intensities of a $(Ta/Si)_{60}$ multilayer: (*a*) a specular scan and (*b*) an off-specular scan with an offset angle of 0.1°. Solid lines represent the results of the fitting.

The off-specular scan intensities of Fig. 1(*b*) show RDS peaks at 2θ values correponding to multilayer Bragg peaks, which implies correlated roughness between different interfaces. Though RDS peaks generate diffuse halos near projected images, the estimated intensities of RDS at multilayer peaks are less than 10^{-3} of those of specular intensities.

Magnitudes of interface roughness have been obtained by analysing non-specular reflectivity intensities in the same way as described elsewhere for (Mo/Si) multilayers (Lee *et al.*, 1998). Interface morphologies are assumed to be self-affine and they can be described by a height–height cross-correlaton function between the mth and nth interface, $C_{mn}(r) = \sigma_r^m \sigma_r^n \exp[-(r/\xi_x)2H] \exp[-(|\bar{z}_m - \bar{z}_n|)/\xi_z]$, which was proposed by others (Sanyal *et al.*, 1992). σ_r^m, r, H, ξ_x, ξ_z and $\bar{z}_m$ are the roughness amplitude of the mth interface, the distance in the lateral direction, the roughness exponent representing the jaggedness of the interfaces, the correlation lengths in the lateral direction and the vertical direction, and the average vertical position of the mth interface, respectively. Non-specular reflectivity intensities were calculated using the distorted-wave Born approximation scheme developed for multilayers (Holý & Baumbach, 1994). The values of H and the lateral correlation length, ξ_x, and the vertical correlation length, ξ_z, were estimated as 0.5, 400 Å and 350 Å, respectively, by fitting the measured non-specular intensities. Solid lines represent the results of fitting, which show good agreement with measurements. Magnitudes of interface roughness were estimated to be 1.5 and 2.0 Å for *A*-type and *B*-type interfaces, respectively.

Interdiffusion of the constituent atoms between adjacent layers results in graded interfaces. Intermixing widths of the graded interfaces are another origin of reduced specular intensities while they do not contribute to non-specular intensities. The intermixing width, σ_i, can be obtained from the relation $\sigma_t^2 = \sigma_i^2 + \sigma_r^2$, where σ_t and σ_r represent the interfacial width and interface roughness, respectively. Estimated intermixing widths, which could be related to silicide formation, are 1.74 Å for *A*-type interfaces and 2.34 Å for *B*-type interfaces.

Densities of both kinds of layers were found to be smaller than values of their crystalline phases, and results of transmission-electron-microscopy measurements showed that the layers were amorphous. Since Ta and Si can form silicides, evolution of the interface morphology of the multilayer is anticipated if it is exposed to intense synchrotron radiation for a long period of time. Investigations of annealing effects on the above structural parameters of (Ta/Si) multilayers are in progress and will be reported later.

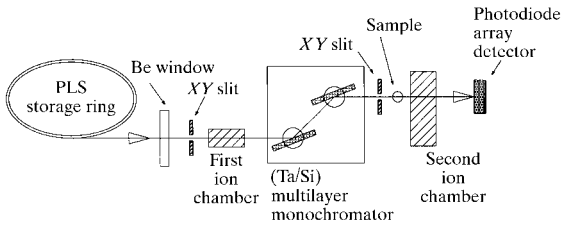

Figure 2
Schematic layout of the optical configuration for the performance test of the $(Ta/Si)_{60}$ multilayer monochromator.

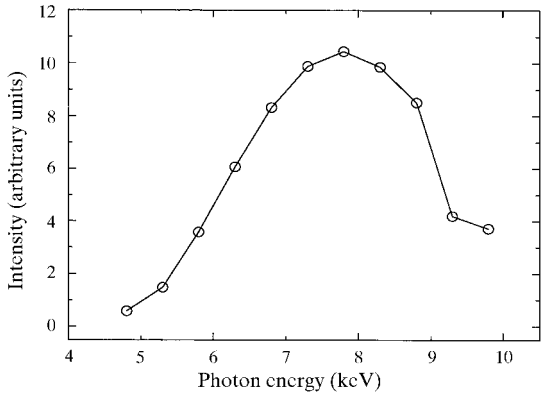

Figure 3
Measured intensities of monochromatic X-rays after the multilayer monochromator.

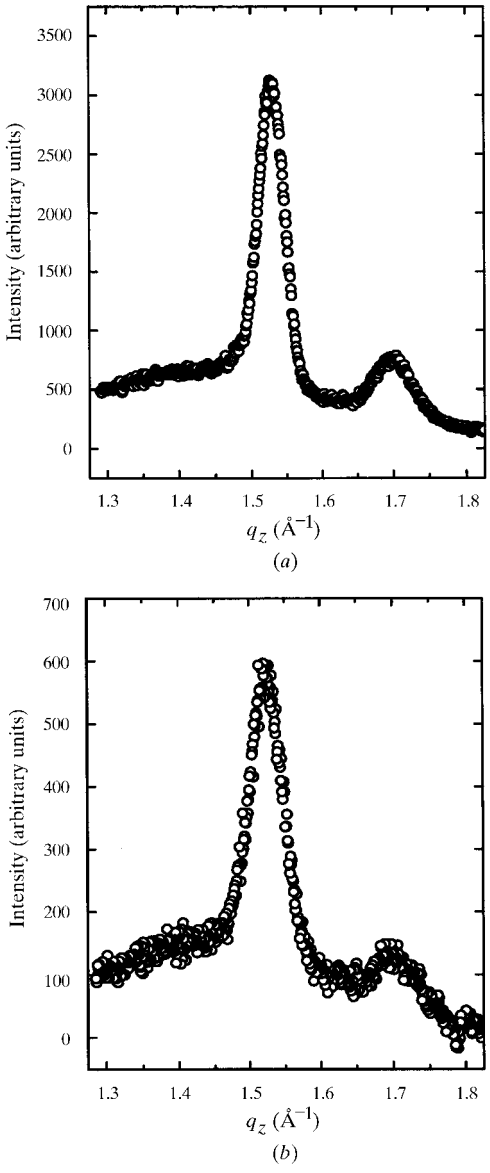

Figure 4
Diffraction patterns of a polyethylene, $-(CH_2)_n-$, measured with different monochromators: (*a*) measured intensities using a focused X-ray beam of λ = 1.608 Å from an Si(111) double-crystal monochromator and (*b*) measured intensities using unfocused X-rays of λ = 1.698 Å from the multilayer monochromator.

3. Performance as a monochromator

A pair of the multilayers were mounted on a double-crystal-monochromator assembly which had been fabricated as a prototype for a monochromator of the PLS 3C2 beamline (Park *et al.*, 1995). Multilayers were held on goniometer heads of two separate Huber 410 goniometers. The position of the second goniometer was controlled by a stepping motor to fix the exit-beam heights when X-ray energy was scanned. The monochromator assembly was tested using white-beam radiation at PLS beamline 1B2 station. Its optical configuration is schematically presented in Fig. 2. An *XY* slit was located after a Be window to intercept unfocused white-beam radiation with horizontal acceptance of 0.4 mrad. Another *XY* slit was placed after the monochromator assembly to define the exit-beam aperture. Two ionization chambers were installed after the slits to monitor the beam intensities. The measured ion currents at different X-ray energies are plotted in Fig. 3. X-ray energies were calibrated using an Si(Li) detector.

Diffraction experiments on a polymer sample, high-density polyethylene (HDPE), were carried out using different monochromators to compare the performances. Diffracted intensities were measured with the same photodiode array detector to avoid the possible ambiguities due to different detectors. Fig. 4 shows background-subtracted diffraction intensities from the same sample taken with different monochromators. Fig. 4(*a*) presents the result taken at 3C2 beamline using 1.608 Å X-rays from an Si(111) double-crystal monochromator. The FWHM of the polyethylene (110) peak is about 0.05 $Å^{-1}$ and a peak corresponding to the (200) plane is clearly observable. Fig. 4(*b*) shows the results of measurements using a pair of $(Ta/Si)_{60}$ multilayers. While the (200) diffraction peak looks like a shoulder, the FWHM of the (110) peak is 0.063 $Å^{-1}$, which is comparable with that of the result with the Si(111) monochromator. This implies that the peak width of the polymer sample is mainly attributed to the sample's intrinsic width and that the multilayer provides an adequate resolution for diffraction experiments on polymers. Since SAXS experiments require less stringent resolutions, the multilayer can be used for SAXS experiments. The weak intensities of the diffracted peak in Fig. 4(*b*) compared with that of Fig. 4(*a*) are mainly due to a low flux of incident X-rays from an unfocused beam.

4. Summary

It has been found that (Ta/Si) multilayers are another promising candidate material for wide-bandpass monochromators for hard X-rays. They show reasonably high reflectances at their multilayer peaks. X-ray reflectivity studies have also been carried out to characterize their interface morphology, and structural parameters related to the morphology were obtained. Further studies of aging effects on their interface morphology and performance are in progress and will be reported later.

Diffraction experiments on an HDPE sample were performed using a pair of $(Ta/Si)_{60}$ multilayers. The data show that a monochromator with the multilayers provides an adequate resolution for experiments on polymer samples.

The experiments at the PLS were supported by the Ministry of Science and Technology (MOST), and Pohang Iron and Steel Co. One of us (KBL) acknowledges support from the Korea Science and Engineering Foundation (96–0702-01–01-3) and Atomic Scale Science Research Center.

References

Deschamps, P., Engström, P., Fiedler, S., Riekel, C., Wakatsuki, S., Høghøj, P. & Ziegler, E. (1995). *J. Synchrotron Rad.* **2**, 124–131.
Holý, V. & Baumbach, T. (1994). *Phys. Rev. B*, **49**, 10668–10676.
Kwak, J. S., Baik, H. K., Kim, J.-H. & Lee, S.-M. (1997). *Appl. Phys. Lett.* **71**, 2451–2453.
Kortright, J. B. & Di Gennaro, R. S. (1989). *Rev. Sci. Instrum.* **60**, 1995–1998.
Lee, D. R., Park, Y. J., Kim, D., Jeong, Y. H. & Lee, K.-B. (1998). *Phys. Rev. B*, **57**, 8786–8789.
Park, B. J., Rah, S.-Y., Park, Y. J. & Lee, K.-B. (1995). *Rev. Sci. Instrum.* **66**, 1722–1724.
Parratt, L. G. (1954). *Phys. Rev.* **95** 359–369.
Phang, Y. H., Kariotis, R., Savage, D. E. & Lagally, M. G. (1992). *J. Appl. Phys.* **72**, 4627–4633.
Salashchenko, N. N., Platonov, Y. Y. & Zuev, S. U. (1995). *Nucl. Instrum. Methods*, A**359**, 114–120.
Sanyal, M. K., Sinha, S. K., Gibaud, A., Satija, S. K., Majkrzak, C. F. & Homma, H. (1992). *Surface X-ray and Neutron Scattering*, edited by H. Zabel & I. K. Robinson, pp. 91–94. Berlin: Springer-Verlag.
Stephenson, G. B. (1988). *Nucl. Instrum. Methods*, A**266**, 447–451.
Ziegler, E. (1995). *Opt. Eng.* **34**, 445–452.